ETH zürich

ETH Library

Optimal economic and environmental design of multi-energy systems

Journal Article

Author(s):
Terlouw, Tom Mike; Gabrielli, Paolo; AlSkaif, Tarek; Bauer, Christian; McKenna, Russell; Mazzotti, Marco

Publication date:
2023-10-01

Permanent link:
https://doi.org/10.3929/ethz-b-000618297

Rights / license:
Creative Commons Attribution 4.0 International

Originally published in:
Applied Energy 347, https://doi.org/10.1016/j.apenergy.2023.121374

This page was generated automatically upon download from the ETH Zurich Research Collection.
For more information, please consult the Terms of use.

Applied Energy 347 (2023) 121374

Contents lists available at ScienceDirect

Applied Energy

journal homepage: www.elsevier.com/locate/apenergy

Optimal economic and environmental design of multi-energy systems

Tom Terlouw [a,b,c,*], Paolo Gabrielli [a,d], Tarek AlSkaif [e], Christian Bauer [c,**], Russell McKenna [b,f], Marco Mazzotti [a]

[a] Institute of Energy and Process Engineering, ETH Zürich, Zürich 8092, Switzerland
[b] Chair of Energy Systems Analysis, Institute of Energy and Process Engineering, ETH Zürich, Zürich 8092, Switzerland
[c] Technology Assessment Group, Laboratory for Energy Systems Analysis, 5232 Villigen PSI, Switzerland
[d] Department of Global Ecology, Carnegie Institution for Science, Stanford, CA, USA
[e] Information Technology Group, Wageningen University and Research, 6706 KN Wageningen, The Netherlands
[f] Laboratory for Energy Systems Analysis, 5232 Villigen PSI, Switzerland

HIGHLIGHTS

- Novel optimization framework for designing multi-energy systems.
- Life cycle environmental burdens and a wide portfolio of technologies considered.
- Strong GHG reductions can be achieved (73%) with a marginal cost increase (18%).
- Multi-energy systems analyses require analyzing non-climate change-related impacts.
- Technology construction phase contributes up to 80% of environmental impacts.

GRAPHICAL ABSTRACT

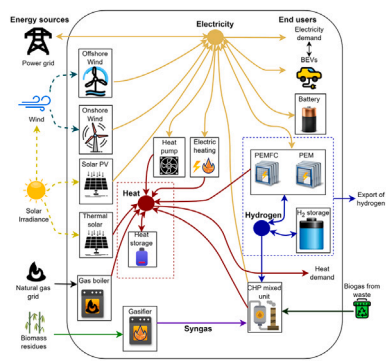

ARTICLE INFO

Keywords:
Multi-energy systems
Life cycle assessment
Techno-economic assessment
Mixed integer linear program
Decarbonization

ABSTRACT

Designing decentralized energy systems in an optimal way can substantially reduce costs and environmental burdens. However, most models for the optimal design of multi-energy systems (MESs) exclude a comprehensive environmental assessment and consider limited technology options for relevant energy-intensive sectors, such as the industrial and mobility sectors. This paper presents a multi-objective optimization framework for designing MESs, which includes life cycle environmental burdens and considers a wide portfolio of technology options for residential, mobility, and industrial sectors. The optimization problem is formulated as a mixed integer linear program that minimizes costs and greenhouse gas (GHG) emissions while meeting the energy demands of given end-users. Whereas our MESs optimization framework can be applied for a large range of boundary conditions, the geographical island Eigerøy (Norway) is used as a showcase as it includes substantial industrial activities. Results demonstrate that, when properly designed, MESs are already cost-competitive with incumbent energy systems, and significant reductions in the amount of natural gas (92%) and GHG emissions (73%) can be obtained with a marginal cost increase (18%). Stricter decarbonization targets incur larger costs. A broad portfolio of technologies is deployed when minimizing GHG emissions and integrating the industrial sector. Environmental trade-offs are identified when considering the construction phase of energy technologies. Therefore, we argue that (i) MES designs and assessments require a thorough life cycle assessment beyond GHG emissions, and (ii) the entire life cycle should be considered when designing MESs, with the construction phase contributing up to 80% of specific environmental impact categories.

* Corresponding author at: Institute of Energy and Process Engineering, ETH Zürich, Zürich 8092, Switzerland.
** Corresponding author.
E-mail addresses: tterlouw@ethz.ch (T. Terlouw), christian.bauer@psi.ch (C. Bauer).

https://doi.org/10.1016/j.apenergy.2023.121374
Received 25 January 2023; Received in revised form 11 May 2023; Accepted 29 May 2023
Available online 23 June 2023
0306-2619/© 2023 The Authors. Published by Elsevier Ltd. This is an open access article under the CC BY license (http://creativecommons.org/licenses/by/4.0/).

Nomenclature

Indices

d	index for days, $d \in \{1, 2, \ldots, D\}$
i	index for technologies, $i \in \{1, 2, \ldots, M\}$
t	index for time steps, $t \in \{1, 2, \ldots, T\}$
z	index for charging schedules, $z \in \{1, 2, \ldots, Z\}$

Sets

$\mathcal{D}$	set of start of each day
$\mathcal{M}$	set of technologies
$\mathcal{T}$	set of time steps
$\mathcal{Z}$	set of charging schedules

Parameters

D	power demand [kW]
b	coefficients from heat pump data [–]
c	price of energy imported [€/kWh]
γ	discount rate [–]
η	efficiency [–]
h	GHG credit for the export of energy [kg CO_2-eq./kWh]
G	GHG emissions generated from construction [kg CO_2-eq.]
g	GHG intensity of energy imported [kg CO_2-eq./kWh]
Π	heat loss coefficient [h^{-1}]
I	irradiation [kW/m^2]
L	lifetime [year]
B	annual amount of biomass available [kWh/year]
W	annual amount of biogas available [kWh/year]
E	daily amount of electricity required for BEVs [kWh/day]
$\overline{\delta}$	maximum power load ratio [–]
$\overline{S}$	maximum size that can be installed [kW(h)]
Θ	temperature parameter [K]
Ω	minimum downtime [h]
$\underline{\delta}$	minimum power load ratio [–]
$\underline{S}$	minimum size that can be installed [kW(h)]
Ψ	minimum uptime [h]
P	renewable energy generation potential [kW/kW_p]
r	revenue from exporting energy [€/kWh]
Λ	self-discharge rate [h^{-1}]
ϕ	time preference for the activation of charging [–]
τ	time to fully charge the storage medium [h]

Superscripts

q	thermal power
gr	grid
h	hydrogen
b	biogas
s	syngas
p	power capacity
om	operation and maintenance
op	fuel for operation
an	annual totals
inst	installation
rep	replacement

Variables

a	binary variable for technology selection [–]
e	energy stored in energy storage technologies [kWh]
f	input power of a technology [kW]
p	output power of a technology [kW]
s	size of a technology [kW(h)]
$\tilde{s}$	auxiliary variable [kW]
u	power imported from grid [kW]
v	power exported to grid [kW]
x	on/off status of conversion and storage technologies [–]
y	startup status of conversion technologies [–]
z	shutdown status of conversion technologies [–]

Indicators

C	annual costs [€/year]
G	annual GHG emissions [kg CO_2-eq./year]

1. Introduction

Limiting global warming to 2 °C requires an immediate transformation of the global energy system [1–3]. More specifically, the energy system is transforming towards decentralized energy systems to integrate distributed renewable energy sources with various flexibility options, to ensure a reliable and sustainable operation of the overall energy system [1,4,5]. Multi-energy systems (MESs) are a promising approach to increase the flexibility, energy security, and reliability of decentralized energy systems, with the ultimate goal to improve their overall economic and environmental performance [6,7]. MESs comprise different energy carriers and sources, such as hydrogen, heat, syngas, biogas, (renewable) electricity, and natural gas. Furthermore, they include multiple energy storage technologies, suited for both short-term (*e.g.*, batteries) and long-term energy storage (*e.g.*, hydrogen storage), to balance the daily and seasonal fluctuations of renewable electricity generation, such as solar photovoltaic (PV) and wind electricity [4].

Energy storage systems are a well-known solution to balance the intermittent nature of renewable energy sources, hence contributing to the overall system flexibility and self-sufficiency of MESs [8,9]. Battery energy storage systems usually provide sufficient energy storage capacity for smaller MESs or community energy systems [10–12]. However, batteries are typically sub-optimal for larger MESs [13,14], or for energy systems that integrate substantial industrial activities, since they require larger (seasonal) energy storage mediums [8,9]. Further, MESs most likely integrate industrial activities that require high-temperature heat, for example on geographical islands [15]. For this reason, MESs typically integrate alternative energy storage systems and energy carriers, such as hydrogen (storage) and syngas. While MESs offer many design options, they are subjected to location-specific constraints and boundary conditions.

To explore optimal solutions within the feasible design space, optimization algorithms are applied to prevent sub-optimal system design and operation as well as to determine trade-offs between economic and environmental objectives [10,13]. To date, several relevant optimization algorithms have been proposed to determine the optimal design of MESs. Gabrielli et al., [13] proposed a mixed integer linear program (MILP) to optimally design and operate MESs with long-term hydrogen storage. The system was optimized on total costs and operational greenhouse gas (GHG) emissions for a Swiss case study. Based on this work, Gabrielli et al., [16] developed an optimization and assessment framework for the optimal and robust design of multi-energy systems under weather and demand uncertainty. Later, Petkov and Gabrielli [17] presented a multi-objective optimization problem to design MESs under uncertainty; they provided a comprehensive uncertainty analysis with regard to technology characteristics, input parameters, and climate-related uncertainties with European scope.

Herenčić et al., [18] presented a MILP to design multi-vector energy communities for the decarbonization of geographical islands. Three sub-models – a battery, hydrogen, and gas model – were proposed and evaluated with regard to total costs, operational CO_2-intensity, and other performance indicators.

These and other similar MES analyses – see for example Refs. [19–30] – exclude or only consider operational GHG emissions, hence neglecting life cycle GHG emissions. However, costs and GHG emissions are generated over the entire life cycle of a MES [31], and GHG emissions from (for example) the construction of technologies can have a significant environmental burden [12,31]. Further, GHG emissions are only one of the relevant environmental impacts generated during the supply chain of energy systems. Limiting the analysis to climate change impacts could result in an unexplored environmental burden shifting, and potentially lead to severe burdens on other environmental impact categories when a global scale-up is considered. Thus, a comprehensive environmental assessment is required to determine environmental trade-offs [12,32,33]. Indeed, Reinert et al. proposed a linear program [33] and a MILP [32] to design energy systems based on costs and life cycle environmental impacts considering different spatial scales. In their work, however, they reduced the time complexity of the optimization problem and failed to capture (i) the competition between short- and long-term energy storage, and (ii) technology-specific constraints that are relevant for coupling the residential, industrial, and mobility sectors. Finally, all previous MES studies focused on low-temperature heat provision and excluded the integration of high-temperature heat requirements from the industry sector.

Hence, an optimization framework that (i) includes both techno-economic and environmental life cycle considerations for the optimal MES design, (ii) integrates the residential, mobility, and the industrial sector, and (iii) considers a long-term time horizon to include seasonal energy storage, is missing. To fill this gap, this work presents a novel optimization framework to minimize costs and GHG emissions as objectives during the entire life cycle of decentralized MESs, considering both low- and high-temperature heat provision for the residential, industrial, and mobility sector. The main novelty of this work is therefore the integration of life cycle assessment (LCA) in the optimization framework and the sector coupling between the residential, industrial, and mobility sector on a MES scale. Alongside the objective functions above, the optimal design is evaluated in terms of environmental trade-offs, such as material utilization and land occupation.

Overall, the contributions of this paper can be summarized as follows.

(i) A novel optimization framework is developed to optimally design MESs: the framework decides to install a set of energy technologies considering system costs and GHG emissions. A comprehensive set of energy technologies is considered, covering sector-coupling with personal transport and industry, namely: onshore and offshore wind, solar PV, solar thermal heat, electric heating, natural gas boilers, wood gasification, advanced combined heat and power (CHP) running on low-carbon fuels, heat storage, heat pumps, battery electricity storage, electrolyzers, fuel cells, hydrogen storage, battery electric vehicles (BEVs), and gasoline vehicles.

(ii) Industrial activities requiring high-temperature heat are considered in the optimization framework. High-temperature heat can be supplied by a natural gas boiler or with advanced CHP units, which can use hydrogen, syngas, and biogas in different fuel proportions to generate low-carbon high-temperature heat and electricity.

(iii) Personal transport is considered in the optimization framework, which can be provided with gasoline vehicles or BEVs using different flexible charging schedules (considering different charging behaviors).

(iv) A comprehensive set of potential environmental trade-offs, resulting from the deployment of MESs, are assessed for a case study in Eigerøy (Norway). These include for example material utilization, acidification, human toxicity, ozone depletion, eutrophication, ecotoxicity, water use, and land transformation.

Our optimization approach is general, is formulated in a flexible and modular way, and can be used to optimally design MESs for case-specific boundary conditions. Therefore, it enables policymakers and system designers to select the most cost-effective system design that complies with emissions and environmental limitations.

The structure of this paper is as follows. The novel optimization framework is presented in Section 2. Results for a selected case study are presented and discussed in Section 3. Conclusions are drawn in Section 4.

2. Methodology

First, we describe the considered MES. Next, we present and discuss the required input data, objective function, and constraints of the novel optimization framework. Finally, we provide the data and assumptions for the selected case study.

2.1. System description: MES on a geographical island

Fig. 1 illustrates a MES, installed on a geographical island. In this work, we apply our optimization framework to geographical islands. Geographical islands are isolated and are usually dependent on imported fossil fuels from the mainland, which makes them a particularly interesting case study towards full decarbonization via MESs [18,34,35]. Further, geographical islands usually have higher potential for renewables, due to higher average wind speeds, generally more land available, and proximity to offshore energy resources.

The MES illustrated in Fig. 1 includes multiple energy carriers: biogas, hydrogen, electricity, heat, and syngas (from wood gasification). Here, we consider a wide portfolio of technology options and energy carriers, which should allow for a sector coupling between the residential, industrial, and personal transportation sectors. Limiting the technology portfolio could exclude possibly cost-effective energy technologies, which might decrease the overall MES performance.

Electricity can be delivered with a wide set of locally installed electricity generation technologies (such as wind and solar PV) and, when available, from the power grid. Hydrogen can be produced with a polymer electrolyte membrane (PEM) electrolyzer using electricity, can be stored in pressurized vessels, can be converted in an advanced CHP unit or in a PEM fuel cell (PEMFC), or can be exported for transport (such as trucks) or industrial purposes. We do not consider alkaline and solid oxide electrolyzers, due to their limited operational flexibility [31,36].

An important element in this MES is the advanced CHP unit, which can generate electricity and high-temperature heat using different low-carbon energy sources as fuel: biogas from waste, syngas from wood gasification, and hydrogen from the electrolyzer. Alternatively, residential low-temperature heat can be generated using natural gas boilers, residential solar thermal, fuel cells, electric heaters, and heat pumps. Biogas can, for instance, be delivered from an anaerobic digester while the waste can originate from residential households or the local (fish) industry.

Further, we consider personal transport, including both battery electric vehicles (representing flexible loads) and gasoline vehicles. It is worth noting that the MES in Fig. 1 shows a system layout where all technologies are installed. However, multiple technologies can be, and are usually, excluded in an optimal MES design due to costs, environmental reasons, or location-specific constraints.

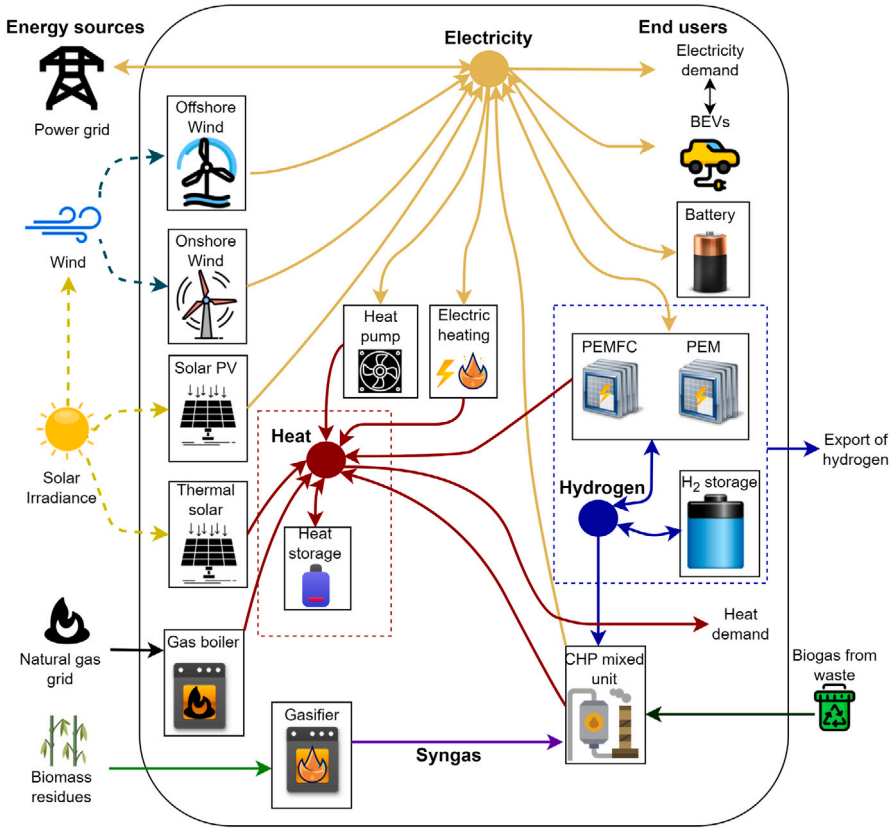

Fig. 1. Technologies considered in the MES on geographical islands. Electricity and heat consumption are both included as well as different storage technologies. In our model, a distinction is made between low- and high-temperature heat, although this is not illustrated in this figure to reduce complexity.

2.2. MILP for optimal design of MESs

The optimal design problem is formulated as a MILP, where binary variables are introduced to model the performance of the conversion units as well as the installation. Though a few nonlinear approaches have been presented [37,38], MILPs are effectively and widely applied to design energy systems [13,39]. In the following, we describe the formulation of the optimization problem in terms of input data, decision variables, constraints, and objective function.

2.2.1. Input data

The most important inputs to the optimization problem are described in the following.

- Weather conditions. Hourly wind speed, solar irradiation (I), and ambient temperature (Θ) are defined based on a typical meteorological year in the location of interest. These are used to determine the output of solar PV, wind power, and residential heat requirements.
- Demand profiles (D) of personal transport, electricity, and heat. The heat demand profile consists of a residential heat demand profile (low-temperature heat) and heat demand required for industrial purposes (high-temperature heat). Aggregated demands are considered for the entire MES under study.
- Techno-economic performance of all technologies. The optimization problem requires cost data, *e.g.,* capital expenditures (CAP-EX), operation and maintenance (O&M), replacement expenditures, and component lifetimes.
- Energy prices. These are the prices of fuels and hourly wholesale electricity prices, which are used to determine the annual system costs.
- Environmental performance. The integration of LCA into the MILP requires life cycle inventories (LCI) of the technologies considered. This can be obtained by either using LCI from an LCA database or by generating foreground LCI.

2.2.2. Decision variables

The following decision variables are returned by the MILP.

- Installed capacity of technologies ($s_i \in \mathbb{R}_+, \forall i \in \mathcal{M}$). The set of technologies ($\mathcal{M}$) is indexed with $i \in \{1, 2, \ldots, M\}$. The binary variable ($a_i \in \{0, 1\}, \forall i \in \mathcal{M}$) is introduced to indicate whether a technology is installed.
- On/off status of selected energy conversion technologies or charging/discharging variable for energy storage technologies ($x_t \in \{0, 1\}, \forall t \in \mathcal{T}$). The set of time steps is defined as $\mathcal{T} = \{1, 2, \ldots, T\}$, where Δt represents the time step. In this work, the binary variable x_t is introduced in the overall assessment period for the wood gasifier, advanced CHP unit, power grid, battery, and heat storage medium.
- Startup status of selected energy conversion technologies ($y_t \in \{0, 1\}, \forall t \in \mathcal{T}$). y_t is equal to "1" when a conversion technology starts-up at t (during one time step), and "0" otherwise. In this work, only the advanced CHP and wood gasification unit are modeled with regard to the startup status.
- Shutdown status of selected energy conversion technologies ($z_t \in \{0, 1\}, \forall t \in \mathcal{T}$). z_t is equal to "1" when a conversion technology is shutdown at t (during one time step), and "0" otherwise. In this work, only the advanced CHP and wood gasification unit are modeled with regard to the shutdown status.
- Input power ($f_{i,t} \in \mathbb{R}_+, \forall t \in \mathcal{T}, \forall i \in \mathcal{M}$) and output power ($p_{i,t} \in \mathbb{R}, \forall t \in \mathcal{T}, \forall i \in \mathcal{M}$), for energy conversion, generation, and storage technologies.

- Energy stored – heat, electricity, and hydrogen – for energy storage technologies ($e_t \in \mathbb{R}_+, \forall t \in \mathcal{T}$).
- Import ($u_t \in \mathbb{R}_+, \forall t \in \mathcal{T}$) and export ($v_t \in \mathbb{R}_+, \forall t \in \mathcal{T}$) of electricity from and to the grid, biomass, and hydrogen. It is worth noting that we only consider hydrogen export and electricity export. In the case of grid-connected systems, locally generated electricity can be exported to the power grid. Further, we consider hydrogen export via outbound transport, since geographical islands might be suited as hydrogen production hubs [31].

2.2.3. Objective function

We determine the optimal design of MESs according to multiple objectives using one year of system operation (T = 8760 h). The first objective, to be minimized, is the total annual cost of the system (C^{an}), considering a time horizon of one year where the energy requirements must be satisfied at each time step. The total annual cost [€/year] includes the annual fuel costs (C^{op}), annualized investments (C^{inv}), annual operation and maintenance costs (C^{om}), and annualized replacements (C^{rep}).

$$\text{minimize} \quad C^{an} = C^{op} + C^{inv} + C^{om} + C^{rep}. \tag{1}$$

Eqs. (2)–(5) show how the underlying cost components are determined.

$$C^{op} = \sum_{i=1}^{M}\sum_{t=1}^{T}(c_t u_{t,i} - r_t v_{t,i})\Delta t, \tag{2}$$

$$C^{inv} = \sum_{i=1}^{M} \frac{\gamma\ (1+\gamma)^{L}}{(1+\gamma)^{L}-1} C_i^{inv}, \tag{3}$$

$$C^{om} = \sum_{i=1}^{M} C_i^{om}, \tag{4}$$

$$C^{rep} = \sum_{i=1}^{M} \frac{\gamma\ (1+\gamma)^{L}}{(1+\gamma)^{L}-1} \frac{C_i^{rep}}{(1+\gamma)^{L_i}}, \tag{5}$$

where c_t and r_t are the prices of imported and exported energy at time t [€/kWh], respectively; γ is the discount rate [–], L_i is the replacement, or lifetime, year of i [year].

Furthermore, we design MESs to minimize their life cycle GHG emissions and other environmental burdens, as we expect that costs for environmental burdens will become more strict due to a wide implementation of policy measures that aim to reduce GHG emissions and other environmental burdens [2,3]. This results in a multi-objective optimization problem, with the environmental objective being described by Eq. (6). The multi-objective optimization problem is solved via the ϵ-constraint method [40,41] .

We account for both environmental impacts from system operation (G^{op}) and from construction of energy technologies (G^{inst}). Therefore, G^{inst} comprises the environmental impact of a technology, which can for example be GHG emissions, land occupation, or materials required to produce and replace a technology. The selected environmental impact category depends on the environmental objective of the optimization problem. It is worth noting that the overall environmental footprint of a technology or energy system should consist of all (or most) environmental impact categories available. However, the importance of separate environmental impact categories in the overall environmental footprint is typically a subjective choice.

$$\text{minimize} \quad G^{an} = G^{op} + G^{inst}. \tag{6}$$

The environmental impacts of the operation and installation are expressed by Eqs. (7) and (8), respectively.

$$G^{op} = \sum_{i=1}^{M}\sum_{t=1}^{T}(g_t u_{t,i} - h_t v_{t,i})\Delta t, \tag{7}$$

$$G^{inst} = \frac{\sum_{i=1}^{M} G_i \frac{L}{L_i}}{L}, \tag{8}$$

where g_t denotes the GHG intensity for the import of energy carriers and electricity at t [kg CO_2-eq./kWh], and h_t denotes a (possible) credit for the export of a fuel at t [kg CO_2-eq./kWh]. G_i are the GHG emissions generated from the production of a technology i [kg CO_2-eq.].

Similar considerations apply for integrating other life cycle environmental burdens either as an objective or as additional constraints.

2.2.4. Constraints

The constraints of the optimization problem can be grouped into two general categories, namely the energy balances of the integrated system and the performance of the individual technologies.

2.2.4.1. Energy balances. Eq. (9) describes the general energy balance applicable for all energy types and for all time steps ($t \in \mathcal{T}$), to ensure that the energy demands (D_t) of all energy carriers are always met. For each energy carrier, the following energy balance must be ensured.

$$\sum_{i\in\mathcal{M}}(u_{i,t} + p_{i,t} - v_{i,t} - f_{i,t}) - D_t = 0 \tag{9}$$

We divide the heat balance into low-temperature heat – required for residential heating purposes (here <100 °C) – and high-temperature heat (>100 °C), which is required for industrial purposes. The former can be provided by heat pumps, sensible heat storage, electric heating, natural gas boilers, solar heat, and fuel cells. The latter can be provided by high-temperature natural gas boilers and advanced CHP units. Moreover, the heat balance excludes heat export ($v = 0, \forall t$), since there is currently no highly-connected heat network available. For the hydrogen balance, we assume that hydrogen can only be generated in the MES and cannot be imported ($u = 0, \forall t$), since a continental hydrogen mobility network is missing today. Also, the hydrogen demand is assumed to be zero ($D = 0, \forall t$), hence hydrogen is only consumed, stored, and produced by technologies within the MES. However, we assume that excess hydrogen production might be exported to the region for industrial activities or for road mobility. Finally, we assume that biomass can be imported to generate syngas, but neither biomass nor syngas can be exported ($v = 0, \forall t$).

2.2.4.2. Installed technologies. The minimum and maximum capacities of technologies in the MES are considered using a binary variable (a). For each technology size (s), the following constraint enforces the minimum ($\underline{S}$) and maximum capacity ($\overline{S}$).

$$\underline{S}_i a_i \le s_i \le \overline{S}_i a_i. \tag{10}$$

It is worth noting that the binary variable a_i is only required for technologies with a minimum allowed installed capacity larger than zero.

2.2.4.3. Connection to the power grid. MESs can be connected to the power grid. In this case, grid power can be imported (u_t) and exported back to the grid (v_t). These power exchanges should respect the maximum power boundaries of the grid ($\overline{S}$). Further, one additional binary variable is introduced (x_t), to prevent simultaneous grid import and export.

$$0 \le u_t \le \overline{S} x_t, \quad \forall t, \tag{11}$$

$$0 \le v_t \le \overline{S}(1 - x_t), \quad \forall t. \tag{12}$$

A smaller capacity of the point of common coupling between the MES and the power grid can be installed when moving towards more self-sufficient systems. Such grid capacity (s^{gr}) is determined via the following equations.

$$0 \le u_t \le s^{gr}, \quad \forall t, \tag{13}$$

$$0 \le v_t \le s^{gr}, \quad \forall t. \tag{14}$$

Note that a value of $s^{gr} = 0$ implies no grid connection, hence a completely self-sufficient MES. Similar constraints can be imposed for the connection with the natural gas grid, to obtain MESs operating without natural gas.

2.2.4.4. Renewable electricity generators. We consider solar PV, onshore wind, and offshore wind as renewable electricity generators. Annual solar PV, onshore wind, and offshore wind power generation profiles are pre-determined (generally denoted by P_t, please refer to the supplementary information for this procedure), and their electricity generation (p_t) is expressed as:

$$p_t \leq \mathrm{P}_t s, \quad \forall t, \tag{15}$$

where the inequality constraint indicates the possibility of curtailing generation. It is worth noting that the amount of curtailed electricity is the difference between the ideal electricity generation (no curtailment, $\mathrm{P}_t s$) and the actual electricity generation (p_t).

2.2.4.5. Natural gas boilers and electric heating. We consider two different natural gas boilers: one for supplying high-temperature industrial heat and one for supplying low-temperature residential heat. The generated thermal power (p_t) can be determined using the fuel supply (f_t) and the technology-specific conversion efficiency (η).

$$p_t = \eta f_t, \quad \forall t, \tag{16}$$

$$0 \leq f_t \leq s, \quad \forall t. \tag{17}$$

Similar considerations and constraints are implemented for electric heating for residential purposes, where the fuel supply (f_t) is powered by electricity.

2.2.4.6. Solar thermal heat. Solar thermal installations on residential rooftops can provide low-temperature heat to residential households or office buildings. The generated thermal power can be obtained using Eq. (18) [13].

$$p_t = \eta \mathrm{I}_t s, \quad \forall t, \tag{18}$$

where I_t is the hourly irradiation per square meter, and, in this case, s is the rooftop area covered with solar thermal panels. The maximum amount of rooftop area available is constrained by the specific case-study.

2.2.4.7. Advanced combined heat and power (CHP) unit. The advanced CHP unit can utilize hydrogen (f_t^{h}), biogas (f_t^{b}), and syngas (f_t^{s}) as fuel, in different proportions, to produce electrical (p_t) and thermal power (p_t^{q}).

$$f_t = f_t^{\mathrm{h}} + f_t^{\mathrm{b}} + f_t^{\mathrm{s}}, \forall t, \tag{19}$$

$$p_t = \eta f_t, \quad \forall t, \tag{20}$$

$$p_t^{\mathrm{q}} = \eta^{\mathrm{q}} f_t, \quad \forall t. \tag{21}$$

The amount of hydrogen that can be utilized is limited by a maximum hydrogen share in the fuel mix for the selected advanced CHP unit. Here, we assume this share to be approximately 60% in energetic terms based on communication with Aurelia turbines (a provider of the advanced CHP unit). A fuel mixer is required to mix the fuels in the right proportions. Thus:

$$f_t^{\mathrm{h}} \leq 0.6 f_t, \quad \forall t. \tag{22}$$

While natural gas could in principle be added as fuel in the advanced CHP unit, we exclude this possibility to maximize the decarbonization benefits of the advanced CHP unit. However, this can easily be included in our model and comes with no loss of generality. Additional constraints, or adaptations, with regard to fuel mixture limitations, can also be easily introduced in the optimization problem.

Importantly, thermal generators, as well as CHP units, have additional constraints with regard to ramp-up and ramp-down rates (τ), minimum uptimes (Ψ), and downtimes (Ω). To consider this, a binary variable (x_t) is introduced to model the on/off status of the advanced CHP unit. Further, additional requirements in terms of minimum ($\underline{\delta}$) and maximum energy generation ($\overline{\delta}$) shares are specified as:

$$\underline{\delta} s x_t \leq f_t \leq \overline{\delta} s x_t, \quad \forall t. \tag{23}$$

This constraint results in the (apparent) bilinearity between the continuous variable s and the binary variable x. The bilinearity between a continuous and a binary variables can be reformulated via two linear constraints by introducing an auxiliary variable $\widetilde{s}_t = s x_t$ as [42]:

$$\underline{\mathrm{S}} x_t \leq \widetilde{s}_t \leq \overline{\mathrm{S}} x_t, \quad \forall t, \tag{24}$$

$$s - \overline{\mathrm{S}}(1 - x_t) \leq \widetilde{s}_t \leq s, \quad \forall t. \tag{25}$$

The ramp-up rate as well as the minimum up- and down-times constraints are formulated as [43,44]:

$$f_t - f_{t-1} \leq \frac{s}{\tau}, \qquad \forall t, \tag{26}$$

$$f_{t-1} - f_t \leq \frac{s}{\tau}, \qquad \forall t, \tag{27}$$

$$x_t - x_{t-1} = y_t - z_t, \qquad \forall t, \tag{28}$$

$$\sum_{i=t-\Psi+1}^{t} y_i \leq x_t, \qquad \forall t \in [\Psi, T], \tag{29}$$

$$\sum_{i=t-\Omega+1}^{t} z_i \leq 1 - x_t, \qquad \forall t \in [\Omega, T]. \tag{30}$$

Here, Eqs. (26)–(27) are required to ensure the maximum ramp-up rates of the advanced CHP unit while Eq. (28) is a logical constraint. Eq. (29) ensures the minimum uptime period while Eq. (30) ensures the minimum downtime period of the advanced CHP unit.

Note that such constraints are introduced for the advanced CHP and wood gasification unit only, to reduce the complexity of the problem and, thus, to reduce the solving time. If needed, for example, to improve the quality of the results, the same constraints can be introduced for other energy conversion technologies.

2.2.4.8. Electric heat pumps. Air source heat pumps provide heat to residential households. We model heat pumps via an hourly coefficient of performance that quantifies the hourly thermal power generated (p_t) as a function of the electricity consumption (f_t). The coefficient of performance is time-dependent and depends on the ambient temperature, as expressed by the right side of the following equation.

$$p_t = (\mathrm{b}_0 + \mathrm{b}_1 \Delta\Theta_t + \mathrm{b}_2 \Delta\Theta_t^2) f_t, \quad \forall t, \tag{31}$$

$$0 \leq p_t \leq s, \quad \forall t. \tag{32}$$

where b are coefficients quantifying the heat pump performance [45], and $\Delta\Theta_t$ can be calculated from the temperature difference between the heat sink (heat supply temperature) and the heat source (ambient temperature denoted by Θ_t).

2.2.4.9. Battery electricity storage. For the battery electricity storage medium, a similar approach is applied as in Refs. [12,31]. Eq. (33) describes the battery dynamics in terms of energy stored (e_t), with battery charging (f_t), discharging (p_t), and considering a self-discharging factor (Λ).

$$e_t = e_{t-1}(1 - \Lambda \Delta t) + \eta f_t \Delta t - \frac{p_t \Delta t}{\eta}, \quad \forall t. \tag{33}$$

Eqs. (34)–(35) are used to avoid simultaneous charging and discharging of the battery (using binary variable x_t), and to ensure that the charging and discharging is within the boundaries of the battery power capacity (s^{p}). The terms on the right side of Eqs. (34) and (35) are bi-linear and are linearized with similar linear terms as described with Eqs. (24) and (25).

Eq. (36) is introduced to consider the minimum ($\underline{\delta}$) and maximum state of charge ($\overline{\delta}$) of the battery system to prevent increased battery degradation rates [46,47]. Eq. (37) is a global balance (or periodicity constraint [13]) that ensures a repeatable operation of the energy storage across multiple years by enforcing the same amount of energy stored at the start and at the end of the optimization period.

$$0 \leq f_t \leq x_t s^{\mathrm{p}}, \quad \forall t, \tag{34}$$

$$0 \leq p_t \leq (1 - x_t)s^{\mathrm{P}}, \quad \forall t, \tag{35}$$

$$\underline{\delta} s \leq e_t \leq \overline{\delta} s, \quad \forall t, \tag{36}$$

$$e_0 = e_T \tag{37}$$

2.2.4.10. Heat storage. Sensible heat storage is considered. This is modeled by following a similar approach as in Refs. [12,13,48]. The sensible heat storage medium is only considered for residential usage and is generally operated for short-term energy storage (from intra-day to a few days). Eq. (38) describes the heat storage dynamics in terms of energy stored (e_t). The heat loss of the storage tank is considered through a loss factor (Π), where the total heat loss also depends on the outside temperature (Θ_t) and temperature boundaries of the tank ($\overline{\Theta}$ and $\underline{\Theta}$).

$$e_t = e_{t-1}(1 - \Lambda \Delta t) - \Pi Y_t s \Delta t + \eta f_t \Delta t - \frac{p_t \Delta t}{\eta}, \quad \forall t, \tag{38}$$

$$Y_t = \frac{\underline{\Theta} - \Theta_t}{\overline{\Theta} - \underline{\Theta}}, \quad \forall t. \tag{39}$$

In case needed, for example to prevent simultaneous charging and discharging of the storage medium, constraints similar to those of battery storage can be implemented, as with Eqs. (34)–(37).

Additional constraints are introduced to account for minimum and maximum power charging and discharging rates.

$$-\frac{s}{\tau} \leq f_t \leq \frac{s}{\tau}, \quad \forall t, \tag{40}$$

$$-\frac{s}{\tau} \leq p_t \leq \frac{s}{\tau}, \quad \forall t. \tag{41}$$

2.2.4.11. Syngas from wood gasification. Syngas (p_t) can be generated from a gasification unit using woody biomass as fuel (f_t).

$$p_t = \eta f_t, \quad \forall t, \tag{42}$$

$$0 \leq f_t \leq s, \quad \forall t. \tag{43}$$

The wood gasification unit is, however, limited to operation within minimum and maximum power limits, ramp-up, uptime, and downtime periods, modeled with equations similar to Eqs. (23)–(30). Further, biomass is a constrained energy source and is usually limited by its regional availability. This is considered by introducing a constraint on the maximum available biomass (B) on an annual basis. This can be expressed as:

$$\sum_{t=1}^{T} f_t \Delta t \leq \mathrm{B}. \tag{44}$$

Here, the syngas produced is only used as input in the advanced CHP unit, thus:

$$f_t^{\mathrm{s}} = p_t, \quad \forall t. \tag{45}$$

2.2.4.12. Biogas from waste. Biogas from waste can be produced, for example, using an anaerobic digestion unit [15]. The amount of biogas available (f_t^{b}), to be used in the advanced CHP unit, is expressed on a daily basis to avoid the large consumption of biogas during specific time steps. In this case, we assume a daily amount of waste available to subsequently produce biogas (W) from households and the fish industry in the considered region. Here, the biogas is solely used as input in the advanced CHP unit. Overall, biogas production is modeled as:

$$\sum_{t=(d-1)24+1}^{24d} p_t \Delta t \leq \frac{\mathrm{W}}{365}, \quad \forall d \in \mathcal{D}, \tag{46}$$

$$f_t^{\mathrm{b}} = p_t, \quad \forall t. \tag{47}$$

2.2.4.13. Hydrogen production via electrolyzers and re-electrification via fuel cells. Hydrogen (p_t) is considered to be produced by PEM electrolyzers, using electricity (f_t). A constant efficiency is considered, in line with earlier findings [49]:

$$p_t = \eta f_t, \quad \forall t, \tag{48}$$

$$0 \leq f_t \leq s, \quad \forall t. \tag{49}$$

Hydrogen (f_t) can be converted to electricity (p_t) and heat (p_t^{q}) via PEMFCs. This is expressed as follows.

$$p_t = \eta f_t, \quad \forall t, \tag{50}$$

$$p_t^{\mathrm{q}} = \eta^{\mathrm{q}} f_t, \quad \forall t, \tag{51}$$

$$0 \leq f_t \leq s, \quad \forall t. \tag{52}$$

2.2.4.14. Hydrogen storage. For the hydrogen storage medium, a similar approach is applied as in Ref. [13]. Eq. (53) describes the hydrogen storage dynamics in terms of energy stored (e_t) as well as power charged and discharged. It is worth noting that there are no energy losses considered during charging and discharging, however, they are considered by applying a lower conversion efficiency for the electrolyzer and the fuel cell in Eq. (48) and (50), respectively. In this situation, the charging and discharging power can be modeled with one variable only (which can be negative). This allows avoiding the introduction of an additional binary variable to prevent simultaneous charging and discharging of hydrogen storage.

$$e_t = e_{t-1} + p_t \Delta t, \quad \forall t. \tag{53}$$

Additional constraints are introduced, similar to Eqs. (36)–(37) and to Eqs. (40)–(41), to limit the amount of hydrogen storage within the installed energy storage capacity, to ensure a yearly energy periodicity, and to respect the maximum charging and discharging rates.

2.2.4.15. Personal transport: battery electric and gasoline vehicles. We consider two different transport modes to meet personal transport requirements: gasoline vehicles and BEVs. The following constraints are active for the integration of BEVs.

First, the BEV charging must respect the maximum ($\overline{\mathrm{S}}$) and minimum power charging boundaries ($\underline{\mathrm{S}}$), considering the total number of BEVs in a specific charging schedule (z). A set ($\mathcal{Z}$) of binary charging schedules for BEVs ($\phi_{t,z}$) are implemented to respect the time preferences for BEV charging, see Section A.2 of the SI for the considered charging schedules. The charging schedules are evenly distributed over the number of households that drive a BEV.

$$\frac{1}{Z}\underline{\mathrm{S}}\phi_{t,z} \leq p_{t,z} \leq \frac{1}{Z}\overline{\mathrm{S}}\phi_{t,z}, \quad \forall t, z, \tag{54}$$

where $z \in \{1, 2, \ldots, Z\}$ is the index of charging schedules of BEVs.

Second, the daily amount of electricity required to charge BEV (E) must be satisfied during each day of the simulation period, thus, for each charging schedule the following constraints are introduced:

$$\sum_{t=(d-1)24+1}^{24d} p_{t,z} \Delta t = \frac{1}{Z}\mathrm{E}, \quad \forall d \in \mathcal{D}. \tag{55}$$

The optimal shares of gasoline vehicles and BEVs, to meet the overall energy demand for mobility, are decision variables in our MILP problem. Other personal transport modes can be easily introduced into the model.

2.3. Data and assumptions

2.3.1. Techno-economic data

Capital expenditures (CAPEX), fuel costs, fixed O&M, and lifetimes of technologies are provided in Table 1. Additional techno-economic data and assumptions are given in Section B.1 of the SI. The general project lifetime is set to 30 years of system operation and the discount rate to 7% [31]. The collection of weather data and the modeling of wind and solar PV are performed using different Python packages, see Section A.1 of the SI [50–53]. Figures of weather conditions and the procedure for the generation profiles are also provided in Section A of the SI. We introduce a sensitivity analysis in Section 3.3 on potentially influencing parameters for a cost optimization, such as weather conditions, energy demand, discount rates, CAPEX, fixed O&M, fuel prices, and lifetimes.

Table 1
Techno-economic parameters quantifying the performance of conversion and storage technologies. The processing of residential waste to biogas is assumed to be burden-free and with a cost of 0.05 €/kWh biogas [54]. The natural gas price assumed is 0.07 €/kWh [15]. The unit for solar thermal investments is €/m^2.

Technology	Sector	C^{inv} [€/kW(h)]	C^{om}	L [year]	η	η_q	δ^{min}	δ^{max}	τ [h]	Λ [h^{-1}]	Π [h^{-1}]	Ψ [h]	Ω [h]	Refs.
Generation														
Solar PV		800	0.02	30										[36]
Onshore wind		1300	0.025	27										[31,36,55]
Offshore wind		2700	0.025	27										[31,36,55]
Solar thermal	residential	500	0.02	25	0.65									[13]
Storage														
Battery electricity	energy	200	0.02	13	0.91		0.035	0.965		0.00054				[31,36]
	power	150	0.02	20										[31,36]
Hydrogen		10	0.02	23	1		0	1	4					[13,17]
Heat	residential	100	0.02	24	0.81		0	1	4	0.0075	0.001			[12,13,17]
Conversion														
Electrolyzer		1100	0.02	7	0.57		0	1						[31,36,56]
Fuel cell		1700	0.04	14	0.5	0.34	0	1						[13,17]
Gas boiler	industrial	100	0.03	20	0.98		0	1						[13,17]
	residential	400	0.03	20	0.9		0	1						[18,57]
Heat pump	residential	1500	0.01	19			0	1						[12,57–59]
Electric heating	residential	1000	0	30	1		0	1						[60,61]
Wood gasification	industrial	1400	0.03	30	0.84		0.1	1	1			8	8	[15]
Mixed CHP	industrial	1400	0.05	20	0.4	0.5	0.05	1	1			8	8	[15]
Road transport		C^{inv} [k€/unit]												
BEVs	residential	48	0.01	17										[62,63]
Gasoline	residential	32	0.03	17										[62]

2.3.2. Environmental data: LCA and inventory

An LCA approach is used to determine environmental burdens of MESs. LCA is a methodology to quantify all environmental burdens over the entire lifetime of a product or service. We apply an attributional LCA approach using background LCA data from ecoinvent 3.9.1 using the '*Allocation, cut-off by classification*" system model [64,65]. Brightway2 is used to calculate the LCA results [66]. LCI data of the energy technologies and energy carriers considered is provided in Section B.2 of the SI. The IPCC 2021 GWP100 environmental impact category has been selected to quantify climate change impacts. Further, we consider all other environmental impact categories of the Environmental Footprint (EF) method "EF v3.1" (except climate change related categories) [67], they are reported in Section B.2 of the SI. We determine the total amount of land transformed, in square meters for the installation of the MES, by aggregating all biosphere flows with "Transformation, from...".

2.4. Case study and the reference system: Eigerøy

The optimization problem is applied to design a MES for the geographical island Eigerøy in Norway. Eigerøy is an island with approximately 2,500 inhabitants at the coastline in the South-West of Norway. The island has a 20–30 MW grid connection with the mainland, here assumed to be 22.5 MW [15,68]. Eigerøy is connected with a bridge to the main land, which allows road and energy transport from and to the island. It is worth noting that the GHG intensity of the Norwegian grid electricity is very low (about 30 gCO_2/kWh of electricity traded [64]), due to a high share of hydropower in the grid electricity mix. The main energy consumer within this geographical island is the fish industry (Prima Protein, located at the harbor), which requires approximately 40 GW h of high-temperature heat per year. The total annual electricity requirement of the island is around 70 GWh. The heat demand of the local fish industry is currently generated with a natural gas boiler. The woody biomass availability on Eigerøy is estimated on 52 t/day with an energy density of 3.5 MWh/t [15,68]. For biogas, 5 W/capita is applied, which is assumed to be generated with the anaerobic digester [69]. Most inhabitants utilize an electrical-based heating system (78%, half of that is assumed to be provided with heat pumps and the other half from electric heating) and the rest of the heating is supplied via wood stovers/biomass boilers in the reference scenario. It is worth noting that there are restrictions on fossil-fuel-based residential heat supply in Norway, therefore, we do not consider residential fossil fuel-burning technologies within the optimization problem for our case study. In the municipality of Eigerøy (Eigersund), personal transport is still dominated by fossil fuels (85%, assumed to be gasoline vehicles), complemented with BEVs (assumed to be 15%). We denote this status quo as the business-as-usual scenario "*BAU*", which represents previously described conditions and costs of the energy system on Eigerøy in 2021.

The island Eigerøy aims to decarbonize its energy system within the next decade [15,34]. This requires a transformation towards low-carbon high-temperature heat in combination with locally produced renewable electricity generation. Energy price data, demand, and energy generation profiles can be found in Section A of the SI. In the following, we list different preferable scenarios, corresponding to the investigated optimizations.

It is worth noting that we consider two scenarios without high-temperature heat, to show the influence of high-temperature heat and the integration of personal transport on the optimal cost design, *i.e.,* scenarios *Cost-Min-Res* and *Cost-Min-Res-M*, respectively. In addition, we provide additional attention for a substantial decrease in terms of GHG emissions subjected to a cost optimization (*i.e*, scenario *Cost-GHG90*), since it is likely that the last part of the Pareto front has a steep slope and, thus, significant GHG reductions can be achieved for a relatively small cost increase. Here, the main focus is on life cycle GHG emissions with the quantification of other environmental impact categories based on the cost and climate change impact objectives. Thus, other environmental burdens are not involved in the optimization problem but are quantified in a post-LCA. These other environmental impact categories are quantified using the optimal outcomes – technology sizes and system operation – of the cost and GHG emission optimization. It is worth noting that objectives can be replaced or additional environmental objectives can be introduced within the problem, which is discussed in Section 3.4.

(1) Scenario "*BAU*": represents the current energy system of Eigerøy in 2021, mainly consuming fossil fuels for heat and low-carbon electricity from the Norwegian grid.

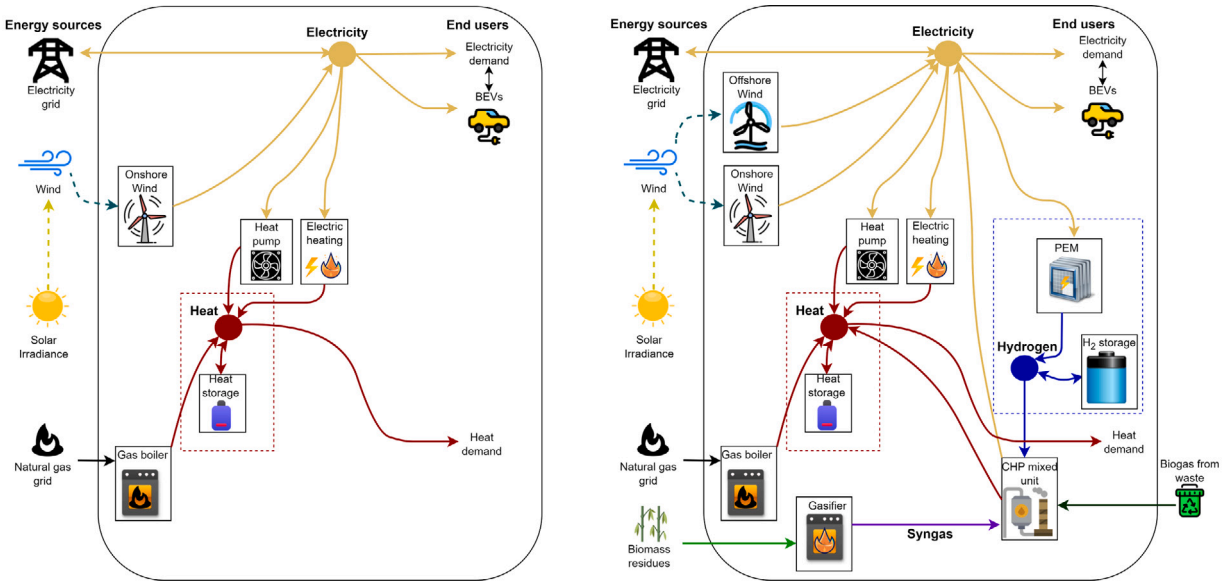

(a) Optimization on costs (*Cost-Min*). (b) Optimization of life cycle GHG emissions (*GHG-Min*).

Fig. 2. MESs installed for a minimization on costs (left) and life cycle GHG emissions (right).

(2) Scenario "*Cost-Min-Res*": is a minimum-cost optimization, which excludes environmental considerations in the objective function and excludes high-temperature heat requirements and personal transport (but includes electricity requirements of the geographical island).
(3) Scenario "*Cost-Min-Res-M*": is a minimum-cost optimization, which excludes environmental considerations in the objective function and excludes high-temperature heat requirements.
(4) Scenario "*Cost-Min*": is a minimum-cost optimization, which excludes environmental considerations in the objective function.
(5) Scenario "*Cost-GHG90*": is a minimum-cost optimization, with a constraint of life cycle GHG emissions to reach a reduction of 90% compared to a cost optimization (that can be obtained on the Pareto front).
(6) Scenario "*GHG-Min*": is an optimization of life cycle GHG emissions, which excludes cost considerations in the objective function.

The model is formulated and solved using the Gurobi (v.10.0) interface in Python (v3.10) [70].

3. Results and discussion

The optimal system designs corresponding to the different scenarios (from Section 2.4) are presented in Section 3.1. Potential environmental trade-offs are discussed in Section 3.2. A sensitivity analysis is presented and discussed in Section 3.3, and further discussion is provided in Section 3.4.

3.1. Results of scenarios

Fig. 2 shows the optimal design of the MES (selected technologies) for a minimum-cost (Scenario 4) and minimum-GHG emissions optimization (Scenario 6), considering all sectors. The cost-optimal design (Fig. 2(a)) still installs GHG-intensive technologies, such as heat generation with natural gas boilers. Interestingly, onshore wind is already a cost-competitive electricity generation technology in Eigerøy. This configuration exhibits a reduction of 14% and 26% in terms of costs and life cycle GHG emissions compared to scenario *BAU*, respectively. In contrast, the minimum-emissions design (Fig. 2(b)) demonstrates a more complex energy system, with a prominent diversification of energy conversion and storage technologies, featuring hydrogen, syngas, and electricity as energy vectors. Compared to scenario *BAU*, the life cycle GHG emissions are reduced by almost 80% (even with a decarbonized power grid). However, this comes at the expense of a 59% increase in annual costs.

Fig. 3 shows the major costs and emissions contributions (stacked bar segments, in different colors) to the overall costs and life cycle GHG emissions for all considered scenarios. Scenarios are reported on the x-axis, the annual costs on the primary y-axis, and the life cycle GHG emissions on the secondary y-axis. For each scenario, the cost contributions are presented with the left bar, while the life cycle GHG emissions are provided with the right bar. The values above the bar indicate the contribution of the investments to the overall costs (left) and the contribution of construction processes to the overall GHG emissions (right). Importantly, the second and third scenario both exclude high-temperature heat, while the second scenario (*Cost-Min-Res*) also excludes personal transport, these scenarios are indicated with the lightgrey shaded area. This allows to determine the impact of the introduction of industrial activities and personal transport in the cost optimal design. In addition, Table 2 reports the sizing of the components in the MES for all scenarios. And lastly, Section C.2 in the SI provides stacked plots showing the annual system operation for the *Cost-Min*, *Cost-GHG90*, and *GHG-Min* scenario.

Furthermore, Fig. 4 provides the Pareto front for the two objectives considered; an optimization of life cycle GHG emissions (on the x-axis) and costs (on the y-axis). Four points are indicated on this figure with a red marker; they correspond to the optimization scenarios provided in Section 2.4. Four small spider graphs are presented in the background of these points, to indicate the environmental performance of these four scenarios, see Fig. 5 for a larger representation and more discussion with regard to these spider graphs. Dotted black lines indicate the relative changes in terms of costs and GHG emissions for different points on the Pareto front compared to the *BAU* scenario. Based on these figures and Table 2, the following considerations can be made.

First, the optimal design largely depends on the integration of different energy sectors, this is illustrated when moving from the left (scenario *BAU*) to the right up to scenario *Cost-Min* in Fig. 3. The

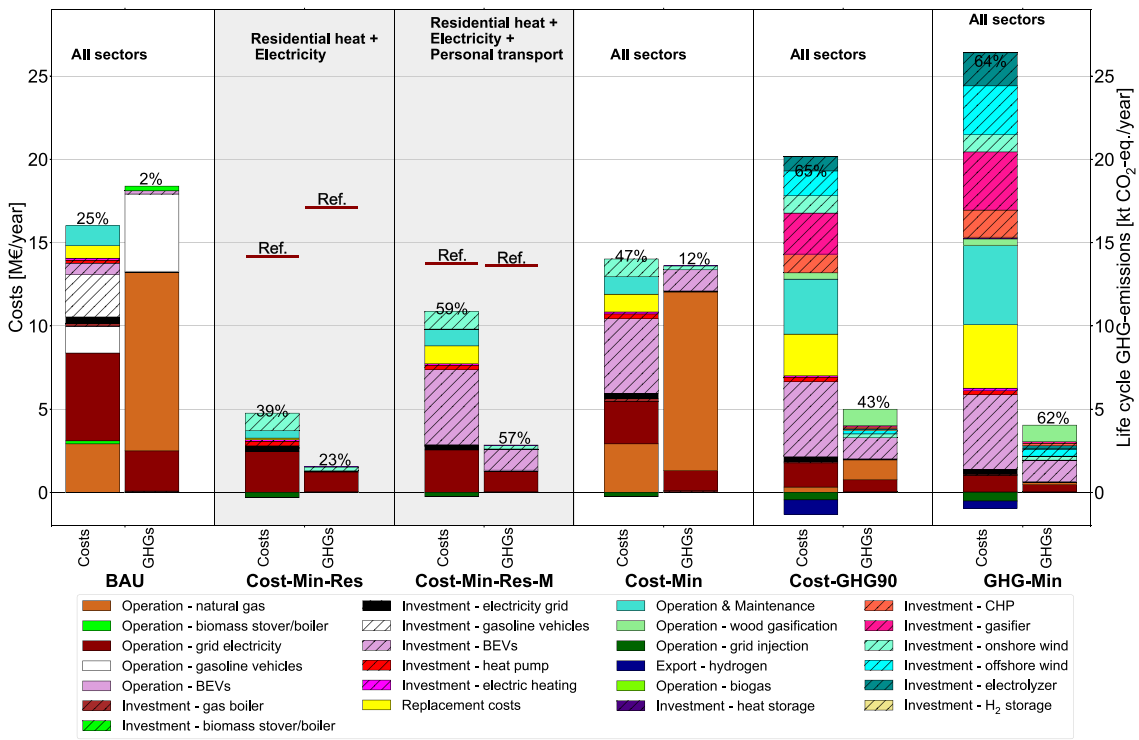

Fig. 3. Major costs and GHG emissions contributions (stacked bar segments, in different colors) for all considered scenarios. Scenarios are reported on the *x*-axis, the annual costs on the primary *y*-axis, and the life cycle GHG emissions on the secondary *y*-axis. The values above the bar indicate the contribution of the investments to the overall costs (left) and the contribution of construction processes to the overall GHG emissions (right). The lightgrey shaded area indicates configurations that exclude industrial heat requirements in the system design. For comparison, the dark red horizontal lines with "Ref." indicate the total costs and GHG emissions when including all sectors (adopted from the BAU scenario) for the scenarios that do not integrate all energy sectors.

Table 2
Techno-economic system performance and design.

Technology	Sub	BAU	Cost-Min-Res	Cost-Min-Res-M	Cost-Min	Cost-GHG90	GHG-Min	
Energy generation								
Solar PV		0.0	0.0	0.0	0.0	0.0	0.0	[MW]
Onshore wind		0.0	10.0	10.0	10.0	10.0	10.0	[MW]
Offshore wind		0.0	0.0	0.0	0.0	6.8	13.4	[MW]
Solar thermal	residential	0.0	0.0	0.0	0.0	0.0	0.0	[ha]
Energy storage								
Battery electricity	energy	0.0	0.0	0.0	0.0	0.0	0.0	[MWh]
	power	0.0	0.0	0.0	0.0	0.0	0.0	[MW]
Hydrogen		0.0	0.0	0.0	0.0	19.3	20.5	[MWh]
Heat	residential	0.0	1.2	1.1	1.1	2.7	12.5	[MWh]
Energy conversion								
Electrolyzer		0.0	0.0	0.0	0.0	9.8	22.4	[MW_f]
Fuel cell		0.0	0.0	0.0	0.0	0.0	0.0	[MW_f]
Gas boiler	industrial	19.4	0.0	0.0	19.4	7.4	7.4	[MW_f]
	residential	0.0	0.0	0.0	0.0	0.0	0.0	[MW_f]
Heat pump	residential	1.5	2.2	2.2	2.2	2.3	2.0	[MW_{th}]
Electric heating	residential	1.5	1.4	1.4	1.4	1.3	1.6	[MW_f]
Wood gasification	industrial	0.0	0.0	0.0	0.0	21.8	31.0	[MW_f]
Mixed CHP	industrial	0.0	0.0	0.0	0.0	24.4	36.0	[MW_f]
Others								
Grid connection		22.5	19.8	19.8	19.8	19.3	18.3	[MW]
Performance								
Total costs		16.0	4.5	10.6	13.8	18.9	25.5	[M€]
Total GHGs		18.4	1.5	2.8	13.6	5.0	4.0	[kt CO_2-eq.]
Grid reliance		n.a.	n.a.	n.a.	−49.1	−71.4	−82.5	[Δ%]
Natural gas reliance		n.a.	n.a.	n.a.	−28.2	−92.0	−99.2	[Δ%]

addition of both the industrial and mobility sector more than doubles the costs and life cycle GHG emissions for the cost-optimal designs. The integration of industrial high-temperature heat results in the installation of substantial different sub-components, such as natural gas boilers, advanced CHP units, and hydrogen-related system components (see Table 2).

Second, Fig. 3 illustrates that the impact of the construction phase can have a substantial contribution to the total environmental impact.

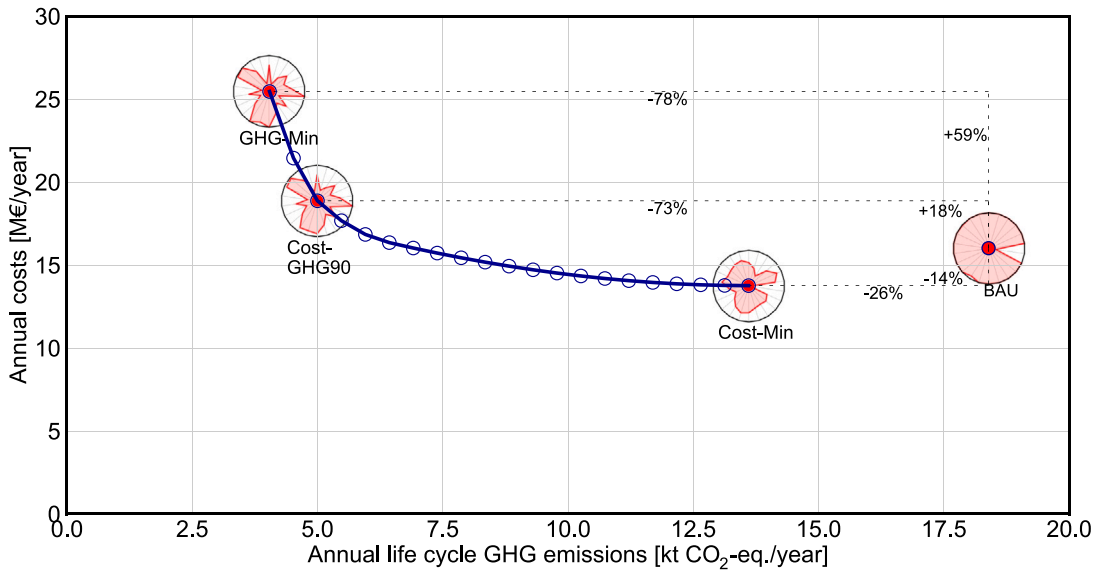

Fig. 4. Pareto front for the trade-off between annual costs and life cycle GHG emissions including all sectors, *i.e.,* the residential, personal transport, and industrial sector in Eigerøy. Spider graphs are provided in the background for four points in this graph, to visualize the impact on other environmental impact categories (see Fig. 5).

More specifically, the construction phase of energy technologies can contribute up to more than 60% of total GHG emissions when designing low-carbon MESs. For other environmental impact categories, this relative contribution can be as high as 80%, for example on human toxicity, metals & minerals, and ozone depletion (see Section C.1 of the SI). Thus, the residual environmental impact from the construction of technologies cannot be neglected in a comprehensive MES analysis.

Third, Fig. 4 logically shows that costs can be mainly reduced for scenarios that consider system costs in the objective function. Life cycle GHG emissions are reduced on the entire Pareto front compared to scenario *BAU*, mainly due to the integration of cost-competitive onshore wind, residential heat pumps, and BEVs. This implies that the energy system installed in scenario *BAU* is both sub-optimal in terms of costs and life cycle GHG emissions.

Fourth, the optimal design is very different among the different scenarios, *i.e.,* optimization scenarios. For example, life cycle GHG emissions can be minimized with *GHG-Min* at the expense of system costs. In this situation, the investments have a large contribution to the overall costs, as the system relies on a high deployment of low-carbon technologies, such as onshore (10 MW) and offshore wind (13 MW), and CHP (36 MW) driven by biogas, hydrogen, and syngas. Moreover, energy storage is deployed in the minimum-emissions design, mostly in the form of hydrogen storage and heat storage for residential households. Battery storage is never deployed, this is further discussed in Section 3.4. For all scenarios, the reliance on the grid electricity and natural gas network is reduced (Table 2).

To illustrate this, the *GHG-Min* and *Cost-GHG90* scenarios (see Table 2) integrate additional energy carriers, energy storage, and intermittent renewables (both onshore and offshore wind) compared to all other scenarios. High-temperature heat is mainly provided with the advanced CHP unit running on low-carbon fuels. The CHP and biomass gasification units do not entirely phase-out natural gas, even when minimizing emissions, because of their minimum-power, downtime, and uptime constraints as well as gas-mixing limitations (see section C.2 in the SI for figures with regard to system operation). In this situation, a natural gas boiler (7 MW) is installed as back-up to provide the rest of the high-temperature industrial heat.

3.2. Environmental trade-offs

Fig. 5 presents the environmental burdens on all considered environmental impact categories for all six optimization scenarios. These are also represented in the background of Fig. 4. The impacts are normalized to the highest impact per category across all optimization scenarios, and are therefore shown on a scale between "0" and "1" (highest possible impact across optimization scenarios).

Fig. 5 shows that scenario *BAU* exhibits the highest environmental burdens compared to all other scenarios. This implies that the environmental impacts, and especially life cycle GHG emissions, can be reduced by properly designing the MES. Besides a significant reduction of life cycle GHG emissions, a cost minimization (*Cost-Min*) also provides a significant reduction in terms of environmental burdens, since some clean energy technologies – for example onshore wind – are already cost-competitive today. For our case study, environmental impact categories that clearly increase towards a cost minimization are climate change, energy resources: non-renewable, ionizing radiation, and ozone depletion. Environmental impact categories that clearly increase towards GHG minimization are land transformation, eutrophication, and some human toxicity impact categories. However, it is worth noting that these trade-offs cannot be generalized as they are typically very case-specific and depend on the location-specific boundary conditions, such as the local climate and hence the potential of renewable energy sources (biomass, solar PV, and wind).

A minimization of life cycle GHG emissions (*GHG-Min*) exhibits higher costs and environmental burdens on a couple environmental impact categories compared to the *BAU* scenario. This implies that an optimization of life cycle GHG emissions results in burden shifting from GHG emissions to other environmental impact categories, such as land occupation (due to harvesting of woody biomass). In short, results imply that a minimization on costs and/or life cycle GHG emissions do not correspond to an equal reduction in terms of the environmental footprint. The environmental footprint must account for other indicators, such as land use, toxicity indicators, and materials.

3.3. Sensitivity analysis: the most influential parameters in a cost minimization

Selected parameters are individually increased and decreased by 10% (a local sensitivity analysis) to determine the most relevant techno-economic parameters for determining the cost of MESs in a cost optimization. The following parameters are selected: electricity and heat demand (residential and industrial), discount rate, grid electricity price, gas price, wood price, investments (capex), lifetimes of

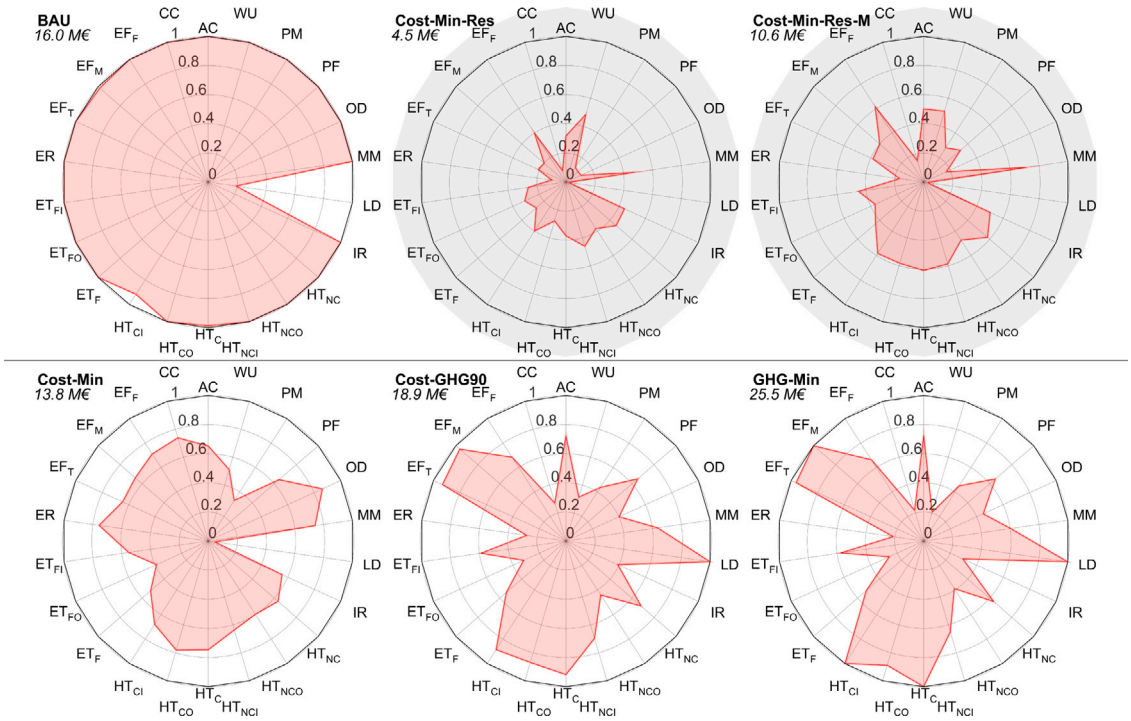

Fig. 5. Spider graph with the different scenarios and associated life cycle environmental burdens on selected normalized environmental impact categories. LD = land transformation. AC = acidification. CC = climate change. ET_F = ecotoxicity: freshwater. ET_{FI} = ecotoxicity: freshwater, inorganics. ET_{FO} = ecotoxicity: freshwater, organics. ER = energy resources: non-renewable. EF_F = eutrophication: freshwater. EF_M = eutrophication: marine. EF_T = eutrophication: terrestrial. HT_C = human toxicity: carcinogenic. HT_{CI} = human toxicity: carcinogenic, inorganics. HT_{CO} = human toxicity: carcinogenic, organics. HT_{NC} = human toxicity: non-carcinogenic. HT_{NCO} = human toxicity: non-carcinogenic, organics. HT_{NCI} = human toxicity: non-carcinogenic, inorganics. IR = ionizing radiation: human health. MM = material resources: metals/minerals. OD = ozone depletion. PM = particulate matter formation. PF = photochemical oxidant formation: human health. WU = water use.

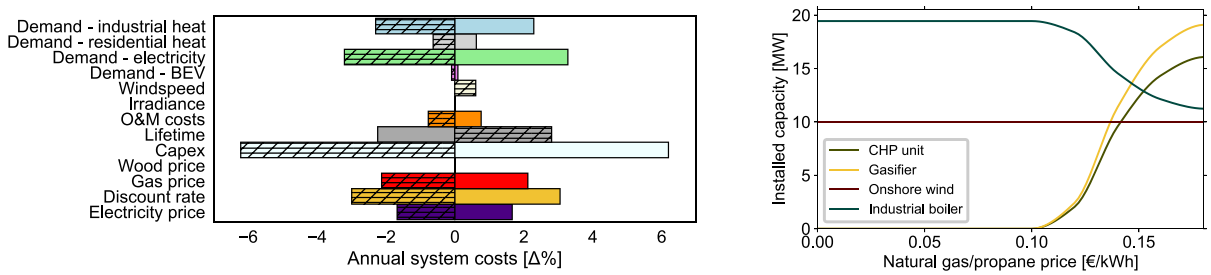

(a) Sensitivity of annual system costs (percentage variation, for a cost optimization) when selected parameters are increased (the non-hatched bars) and decreased by 10% (the hatched bars).

(b) Sensitivity of installed capacities for selected technologies for an absolute increase in natural gas prices.

Fig. 6. Sensitivity analysis on selected parameters, with special attention to natural gas prices.

technologies, O&M costs, average annual solar irradiance, and wind speed.

Fig. 6(a) presents the sensitivity of the annual system cost on the aforementioned parameters, when these parameters are increased and decreased by 10% with respect to their reference value. Fig. 6(b) presents the sensitivity of the system design (installed capacities) on one of the most influential cost parameters for the case study considered: natural gas price. The installed capacities of the following technologies are shown: advanced CHP unit, gasifier, onshore wind, and the industrial boiler driven by natural gas/propane.

Fig. 6(a) shows that an equal increase in terms of capital expenditures has the biggest impact on annual costs for the case study considered. This is mainly explained by the investments required for personal transport. Further, increasing the demand for heat and electricity has substantial impacts. In our case study, the energy demand is highly affected by the local industry. The discount rate is an important parameter and is especially influential in the cost-optimal MES, due to the high requirement of capital expenditures. The price of natural gas is the most influential fuel price in this MES. Currently, natural gas is still comparably cheaper than alternative fuels, and it is therefore chosen as one of the main energy sources in the MES for a cost optimization. An increase of natural gas and grid electricity prices have a significant influence on the annual costs since the operational energy requirements are large and they are still required in addition to the deployment of cost-competitive renewables. An increase of technology lifetimes results in lower annual costs, due to less component replacement expenditures. Fig. 6(b) shows that the advanced CHP unit is already a cost-competitive technology with natural gas/propane prices higher than 0.12 €/kWh, which comes at the expense of the installed capacity of the industrial boiler running on fossil fuels.

3.4. Discussion: limitations, solutions, and future work

Several factors are key to the optimal design of MESs. In the following, we discuss the validity of our results by putting such design factors into perspective with our analysis.

Among the most prevailing issues in the development of optimization algorithms are the trade-offs between complexity, *i.e.*, computational time, and accuracy of the solution, *e.g.*, reliability of the results [71,72]. Optimal design algorithms minimizing environmental objectives tend to have a higher computational burden, due to the integration of a larger set of (low-carbon) energy technologies compared to a cost optimization. In our case, the minimum cost solution (*Cost-Min*) is reached in less than two minutes, the minimum GHG emissions solution (*GHG-Min*) in less than one hour, while introducing a constraint on GHG emissions during a cost minimization increases the solving time by up to eighteen hours (*Cost-GHG90*). This implies that the number and the amount of details in terms of modeling of energy technologies should be evaluated based on the scope and objective of the optimization problem.

This paper focuses on cost and GHG optimization. It is possible to consider other environmental impact categories within our optimization framework, for example, by quantifying their monetary figures or by using additional environmental constraints. However, the integration of additional objectives typically increases the complexity of the optimization problem and might require specific meta-heuristic methods and other subjective choices, such as choosing weighting factors for the set of selected environmental impact categories. The willingness to limit arbitrary choices on the values of the objectives convinced us to focus on costs and GHG emissions as objective functions and to assess environmental burdens through post-optimization analysis.

Within this context, an important aspect concerns the time resolution of the optimization. Here, we use an hourly resolution over a year time horizon to optimally design MESs, which allows considering both short-term (battery) and long-term (hydrogen) storage with seasonal fluctuations. The optimal MES designs that integrate life cycle GHG emissions introduce hydrogen storage to ensure energy available during days with no or low provision of renewable energy supply. Thus, the combination of hourly resolution with a yearly time horizon is necessary to design MESs that deploy multiple energy storage technologies including long-term energy storage [13].

Battery electricity storage is not deployed in our optimal MES designs, which contrasts with some existing literature. This is due to the low capacity factor of solar PV in our case study (which leads to no solar PV capacity installed), comparably high energy discharge losses, higher environmental burdens from construction, and comparably short lifetimes of batteries. Further, very low-carbon electricity can be absorbed from the Norwegian power grid, thus, there is no need to store locally generated renewable electricity with battery electricity storage to ensure the utilization of decarbonized electricity. On the contrary, we do see the installation and operation of hydrogen storage. This is mainly due to two reasons. First, hydrogen can be used as a fuel in the advanced CHP unit for high-temperature heat provision. Therefore, the consideration of high-temperature heat and the presence of the advanced CHP units affect the behavior of hydrogen storage, which is also used for short-term time horizons during periods with large amounts of industrial heat demand (Figure A30 of the SI). Second, hydrogen storage is most suited to compensate for the fluctuations of wind resources, which are predominant in our case study. Overall, hydrogen storage is the better technology option for storing energy for long periods of time (due to its lower self-discharge losses and its lower cost per unit energy stored) and when coupled to industrial requirements and wind energy sources. This is in line with earlier findings presented in Refs. [17,73]. It might be interesting to examine the economic and environmental trade-offs between different energy storage technologies in greater detail, by introducing more energy storage-specific details and technologies for electricity, low-temperature, and high-temperature heat storage, especially at locations with more favorable conditions for solar PV.

We demonstrated that the integration of industrial activities has a significant influence on the optimal MES designs, mainly due to high-temperature heat requirements. In our optimization framework, high-temperature heat can be generated with a natural gas boiler and an advanced CHP unit running on low-carbon fuels. The results showed that a natural gas boiler is selected for the entire high-temperature heat demand in the cost-optimal design, or is deployed to provide backup heat when the advanced CHP unit is installed when GHG emissions are considered in the objective. In reality, more technologies for high-temperature heat provision can be introduced, such as electric boilers running on low-carbon electricity. Such electric boilers can be easily introduced into our optimization framework without introducing much additional complexity, due to their operational flexibility [74]. The integration of electric boilers for high-temperature heat provision might lead to a phase-out of natural gas boilers, thus, could achieve full decarbonization. Alternatively, high-temperature heat storage might avoid the oversizing of technologies and the need for a backup natural gas boiler.

Expanding the system boundaries by including personal transport has a significant influence on costs and total life cycle GHG emissions in our case study, resulting in double costs and life cycle GHG emissions of the system. For simplicity, we only considered home charging and applied wholesale electricity prices for BEV charging, while such charging costs are usually higher for residential consumers. We considered the investments and environmental burdens of the production of vehicles, to be used for personal transportation, in our quantification of costs and overall environmental burdens. Personal transportation is an important component of a MES since BEVs are modeled as a flexible load and hence can absorb renewable electricity generation, however, they come at a cost and environmental burden. Excluding the costs and environmental burdens from the production of vehicles might result in an incomplete understanding of the overall consequences of the integration of transport in a MES. The residential mobility model can be expanded to consider additional charging and fuel infrastructures, vehicle-to-grid, and other vehicles powered by diverse energy sources, such as hydrogen. For a prospective future scenario, for example using the prospective LCA Python package *premise* [75], it might be interesting to examine the integration of other promising energy technologies.

Moreover, we assume perfect knowledge of renewable energy generation, hence neglecting the uncertainty associated with current and future climate conditions. In reality, the variability of future energy generation might affect the economic and environmental potential of MESs [16,76]. It might therefore be interesting to include the stochasticity of renewables into the optimization problem [77,78], though this further increases the complexity and computational efforts. Additionally, a robustness analysis could provide insights into the accuracy and resilience of the optimally designed MES [16].

We focused on economic and environmental indicators to optimally design MESs under certain boundary conditions. Such location-specific boundary conditions are for example related to the energy demand, supply, (available) infrastructure, temperature of heat requirement, and climates. These factors should be considered when applying the model to other case studies, which are planned for follower geographical islands in the future. Considering an even wider technology portfolio could reduce costs and environmental burdens but likely increases the complexity of the optimization problem. In reality, other factors are important to consider when installing a MES. For example, the reliability of the system, and its resilience with respect to uncertain techno-economic scenarios should be considered during the design phase. Moreover, public acceptance and local decision-making, and other socio-economic factors, can hinder the implementation of a low-carbon MES [79,80]. Though such qualitative factors are difficult to include in an optimization framework, they should be considered when

designing a MES with, for example, stakeholder engagement [81]. This implies that our optimization framework can be applied in the early design phase of a MES, however, it should be accompanied by additional analyses. Energy system designers and policymakers can therefore utilize our optimization framework to have a first indication of what costs, life cycle GHG emissions, and environmental burdens can be achieved. Further, we assumed a conservative approach with regard to the export of energy, since we excluded potential environmental credits for energy export for reasons discussed in earlier recent works [12,31].

Increased energy autonomy might avoid the need for expanding the grid capacity as it might reduce system costs, environmental impacts, and could improve the energy security of a geographical island [39,82]. However, this might result in trade-offs and they need to be considered on a case-by-case basis [31,83]. Whilst many studies analyze decentralized energy-autonomous systems, many overlook wider system-level impacts (*e.g.*, considering the energy infrastructure) at the regional and national levels [84]. Hence, our MILP can be used to determine the costs and environmental impacts associated with highly self-sufficient energy systems.

And lastly, the integration of environmental aspects in the MILP offers possibilities to determine the environmental implications of the wider global deployment of MESs. To assess this, the optimization problem can be applied to other decentralized energy systems with different site-specific boundary conditions, such as GHG-intensive power grids and other climate conditions.

4. Conclusions and implications

This paper proposes an optimization framework to optimally design MESs considering a large set of renewable energy generators, storage, and conversion technologies and coupling the residential, mobility, and industrial sectors. The optimization approach is tested on one MES to be installed on a geographical island with substantial industrial activities: Eigerøy (Norway). Our results have significant implications that should be considered in the analysis of low-carbon decentralized energy systems.

First, the construction phase of technologies can have a significant contribution to the environmental impact of a MES. More specifically, the relative share of the construction phase can be up to about 80% for various environmental impact categories, for example metals & minerals, ozone depletion, and human toxicity.

Second, designing MESs with minimization of life cycle GHG emissions does not correspond to an equal reduction in terms of the total environmental footprint. In contrast, minimizing GHG emissions could result in environmental burden shifting, increasing for example land transformation and human toxicity. This implies that energy system designers should consider non-climate change-related impacts in the design phase and that they should extend the system boundaries beyond the operational phase.

Third, expanding the system boundaries beyond the residential sector has a big influence on the optimal design of MESs, especially for industrial activities consuming high-temperature heat. The integration of high-temperature heat in the optimization framework highlights a few salient points. For example, a CHP unit – using a mixture of low-carbon fuels – might be an effective solution to decarbonize MESs with high-temperature heat demands.

Finally, the findings highlight that significant reductions in the amount of natural gas (92%) and GHG emissions (73%) can be obtained with a marginal cost increase (18%). This conclusion is in agreement with previous studies focusing on the residential sector and we generalize it to MESs decarbonizing the residential, mobility, and industrial sectors.

Overall, the implementation of different renewable energy carriers in MESs, with industrial activities, has the potential to substantially reduce life cycle environmental burdens. However, we demonstrate that it is of crucial importance to consider a comprehensive environmental LCA during the design phase, which goes beyond climate change impacts. The integration of life cycle environmental aspects into the optimization framework can indicate preferable outcomes and can possibly avoid environmental burden shifting.

CRediT authorship contribution statement

Tom Terlouw: Conceptualization, Software, Methodology, Formal analysis, Visualization, Writing – original draft. **Paolo Gabrielli:** Conceptualization, Software, Methodology, Writing – review & editing. **Tarek AlSkaif:** Conceptualization, Software, Methodology, Writing – review & editing. **Christian Bauer:** Conceptualization, Supervision, Writing – review & editing. **Russell McKenna:** Writing – review & editing. **Marco Mazzotti:** Supervision, Writing – review & editing.

Declaration of competing interest

The authors declare that they have no known competing financial interests or personal relationships that could have appeared to influence the work reported in this paper.

Data availability

Data will be made available on request.

Acknowledgments

This work has received funding from the European Union's Horizon 2020 Research and Innovation Programme under Grant Agreement No. 957752 (ROBINSON). Further financial support has been provided by PSI's Energy System Integration platform. We thank all partners involved in the ROBINSON H2020 project. Specifically, we thank Steinar Aamodt (Prima Protein) for providing and publishing their energy demand data. We further thank Toni Hartikainen (Aurelia) and Edward Kennedy-George (Aurelia) for feedback and data provision with regard to their gas turbine. And finally, we thank Peter Breuhaus (NORCE) for his continuous support and feedback.

Supplementary data

Supplementary material related to this article can be found online at https://doi.org/10.1016/j.apenergy.2023.121374.

References

[1] IEA. Net Zero by 2050 - A roadmap for the global energy sector. Net Zero By 2050, IEA; 2021, p. 1–224.
[2] Shukla PR, Skea J, Slade R, Al Khourdajie A, van Diemen R, McCollum D, et al., editors. Climate change 2022: Mitigation of climate change. Contribution of working group III to the sixth assessment report of the intergovernmental panel on climate change. Technical report, IPCC; 2022.
[3] IPCC. Climate change 2021: The physical science basis. Contribution of working group I to the sixth assessment report of the intergovernmental panel on climate change. Technical report, Cambridge University Press, IPCC; 2021, [Masson-Delmotte, V., P. Zhai, A. Pirani, S. L. Connors, C. Péan, S. Berger, N. Caud, Y. Chen, L. Goldfarb, M. I. Gomis, M. Huang, K. Leitzell, E. Lonnoy, J. B. R. Matthews, T. K. Maycock, T. Waterfield, O. Yelekçi, R. Yu and B. Zhou (eds.)]. Cambridge University Press. [In Press].
[4] IEA. Renewables 2020 - Analysis and forecast to 2025. Technical report, IEA; 2020, p. 1–172.
[5] Rissman Jeffrey, Bataille Chris, Masanet Eric, Aden Nate, Morrow III William R, Zhou Nan, et al. Technologies and policies to decarbonize global industry: Review and assessment of mitigation drivers through 2070. Appl Energy 2020;266:114848.
[6] Guelpa Elisa, Bischi Aldo, Verda Vittorio, Chertkov Michael, Lund Henrik. Towards future infrastructures for sustainable multi-energy systems: A review. Energy 2019;184:2–21.
[7] Mancarella Pierluigi. MES (Multi-Energy Systems): An overview of concepts and evaluation models. Energy 2014;65:1–17.

[8] Krishan Om, Suhag Sathans. An updated review of energy storage systems: Classification and applications in distributed generation power systems incorporating renewable energy resources. Int J Energy Res 2019;43(12):6171–210.

[9] Olabi AG, Onumaegbu C, Wilberforce Tabbi, Ramadan Mohamad, Abdelkareem Mohammad Ali, Al-Alami Abdul Hai. Critical review of energy storage systems. Energy 2020;118987.

[10] Terlouw Tom, AlSkaif Tarek, Bauer Christian, van Sark Wilfried. Multi-objective optimization of energy arbitrage in community energy storage systems using different battery technologies. Appl Energy 2019;239:356–72.

[11] Parra David, Swierczynski Maciej, Stroe Daniel I, Norman Stuart A, Abdon Andreas, Worlitschek Jörg, et al. An interdisciplinary review of energy storage for communities: Challenges and perspectives. Renew Sustain Energy Rev 2017;79:730–49.

[12] Terlouw Tom, AlSkaif Tarek, Bauer Christian, Mazzotti Marco, McKenna Russell. Designing residential energy systems considering prospective costs and life cycle GHG emissions. Appl Energy 2023;331:120362.

[13] Gabrielli Paolo, Gazzani Matteo, Martelli Emanuele, Mazzotti Marco. Optimal design of multi-energy systems with seasonal storage. Appl Energy 2018;219:408–24.

[14] Gabrielli P, Poluzzi A, Kramer GJ, Spiers C, Mazzotti M, Gazzani M. Seasonal energy storage for zero-emissions multi-energy systems via underground hydrogen storage. Renew Sustain Energy Rev 2020;121.

[15] ROBINSON. Smart integration of local energy sources and innovative storage for flexible, secure and cost-efficient energy supply ON industrialized islands. 2020.

[16] Gabrielli Paolo, Fürer Florian, Mavromatidis Georgios, Mazzotti Marco. Robust and optimal design of multi-energy systems with seasonal storage through uncertainty analysis. Appl Energy 2019;238:1192–210.

[17] Petkov Ivalin, Gabrielli Paolo. Power-to-hydrogen as seasonal energy storage: An uncertainty analysis for optimal design of low-carbon multi-energy systems. Appl Energy 2020;274:115197.

[18] Herenčić Lin, Melnjak Matija, Capuder Tomislav, Andročec Ivan, Rajšl Ivan. Techno-economic and environmental assessment of energy vectors in decarbonization of energy islands. Energy Convers Manage 2021;236:114064.

[19] Marocco P, Ferrero D, Gandiglio M, Ortiz MM, Sundseth K, Lanzini A, et al. A study of the techno-economic feasibility of H2-based energy storage systems in remote areas. Energy Convers Manage 2020;211:112768.

[20] Zhao Guangling, Nielsen Eva Ravn, Troncoso Enrique, Hyde Kris, Romeo Jesús Simón, Diderich Michael. Life cycle cost analysis: A case study of hydrogen energy application on the Orkney Islands. Int J Hydrogen Energy 2019;44(19):9517–28.

[21] Marocco Paolo, Ferrero Domenico, Martelli Emanuele, Santarelli Massimo, Lanzini Andrea. An MILP approach for the optimal design of renewable battery-hydrogen energy systems for off-grid insular communities. Energy Convers Manage 2021;245:114564.

[22] Li Bei, Roche Robin, Miraoui Abdellatif. Microgrid sizing with combined evolutionary algorithm and MILP unit commitment. Appl Energy 2017;188:547–62.

[23] Li Bei, Roche Robin, Paire Damien, Miraoui Abdellatif. Sizing of a stand-alone microgrid considering electric power, cooling/heating, hydrogen loads and hydrogen storage degradation. Appl Energy 2017;205:1244–59.

[24] Rullo P, Braccia L, Luppi P, Zumoffen D, Feroldi D. Integration of sizing and energy management based on economic predictive control for standalone hybrid renewable energy systems. Renew Energy 2019;140:436–51.

[25] Pombo Daniel Vázquez, Martinez-Rico Jon, Marczinkowski Hannah M. Towards 100% renewable islands in 2040 via generation expansion planning: The case of São Vicente, Cape Verde. Appl Energy 2022;315:118869.

[26] Ma Tengfei, Wu Junyong, Hao Liangliang, Lee Wei-Jen, Yan Huaguang, Li Dezhi. The optimal structure planning and energy management strategies of smart multi energy systems. Energy 2018;160:122–41.

[27] Good Nicholas, Ceseña Eduardo A Martínez, Zhang Lingxi, Mancarella Pierluigi. Techno-economic and business case assessment of low carbon technologies in distributed multi-energy systems. Appl Energy 2016;167:158–72.

[28] Karmellos M, Mavrotas G. Multi-objective optimization and comparison framework for the design of distributed energy systems. Energy Convers Manage 2019;180:473–95.

[29] Maroufmashat Azadeh, Sattari Sourena, Roshandel Ramin, Fowler Michael, Elkamel Ali. Multi-objective optimization for design and operation of distributed energy systems through the multi-energy hub network approach. Ind Eng Chem Res 2016;55(33):8950–66.

[30] Petkov Ivalin, Gabrielli Paolo, Spokaite Marija. The impact of urban district composition on storage technology reliance: trade-offs between thermal storage, batteries, and power-to-hydrogen. Energy 2021;224:120102.

[31] Terlouw Tom, Bauer Christian, McKenna Russell, Mazzotti Marco. Large-scale hydrogen production via water electrolysis: Techno-economic and environmental assessment. Energy Environ Sci 2022;15:3583–602.

[32] Reinert Christiane, Schellhas Lars, Frohmann Julia, Nolzen Niklas, Tillmanns Dominik, Baumgärtner Nils, et al. Combining optimization and life cycle assessment: Design of low-carbon multi-energy systems in the SecMOD framework. In: Combining optimization and life cycle assessment: design of low-carbon multi-energy systems in the SecMOD Framework. Elsevier; 2022, p. 1201–6.

[33] Reinert Christiane, Schellhas Lars, Mannhardt Jacob, Shu David, Kämper Andreas, Baumgärtner Nils, et al. SecMOD: An open-source modular framework combining multi-sector system optimization and life-cycle assessment. Front Energy Res 2022;10:884525.

[34] ROBINSON. ROBINSON. 2021.

[35] Gabderakhmanova Tatiana, Marinelli Mattia. Multi-energy system demonstration pilots on geographical Islands: An overview across Europe. Energies 2022;15(11):3908.

[36] Bauer Christian, Heck T, Schneider S, Sanjaykumar H, Terlouw T, Treyer K, et al. Electricity storage and hydrogen: Technologies, costs and environmental burdens. Technical report, PSI, Paul Scherrer Institut; 2022.

[37] Moretti Luca, Manzolini Giampaolo, Martelli Emanuele. MILP and MINLP models for the optimal scheduling of multi-energy systems accounting for delivery temperature of units, topology and non-isothermal mixing. Appl Therm Eng 2021;184:116161.

[38] Gabrielli Paolo, Acquilino Alberto, Siri Silvia, Bracco Stefano, Sansavini Giovanni, Mazzotti Marco. Optimization of low-carbon multi-energy systems with seasonal geothermal energy storage: The Anergy Grid of ETH Zurich. Energy Convers Manag: X 2020;8:100052.

[39] Klemm Christian, Vennemann Peter. Modeling and optimization of multi-energy systems in mixed-use districts: A review of existing methods and approaches. Renew Sustain Energy Rev 2021;135:110206.

[40] Ehrgott Matthias. Multicriteria optimization, vol. 491. Springer Science & Business Media; 2005.

[41] Chircop Kenneth, Zammit-Mangion David. On-constraint based methods for the generation of Pareto frontiers. J Mech Eng Autom 2013;3(5):279–89.

[42] Glover Fred. Improved linear integer programming formulations of nonlinear integer problems. Manage Sci 1975;22(4):455–60.

[43] Knueven Ben, Ostrowski Jim, Watson Jean-Paul. Exploiting identical generators in unit commitment. IEEE Trans Power Syst 2017;33(4):4496–507.

[44] Carrion M, Arroyo JM. A computationally efficient mixed-integer linear formulation for the thermal unit commitment problem. IEEE Trans Power Syst 2006;21(3):1371–8.

[45] Fischer David, Wolf Tobias, Wapler Jeannette, Hollinger Raphael, Madani Hatef. Model-based flexibility assessment of a residential heat pump pool. Energy 2017;118:853–64.

[46] Terlouw Tom, Zhang Xiaojin, Bauer Christian, Alskaif Tarek. Towards the determination of metal criticality in home-based battery systems using a Life Cycle Assessment approach. J Clean Prod 2019;221:667–77.

[47] Schmidt Tobias S, Beuse Martin, Zhang Xiaojin, Steffen Bjarne, Schneider Simon F, Pena-Bello Alejandro, et al. Additional emissions and cost from storing electricity in stationary battery systems. Environ Sci Technol 2019;53(7):3379–90.

[48] Steen David, Stadler Michael, Cardoso Gonçalo, Groissböck Markus, DeForest Nicholas, Marnay Chris. Modeling of thermal storage systems in MILP distributed energy resource models. Appl Energy 2015;137:782–92.

[49] Gabrielli Paolo, Gazzani Matteo, Mazzotti Marco. Electrochemical conversion technologies for optimal design of decentralized multi-energy systems: Modeling framework and technology assessment. Appl Energy 2018;221:557–75.

[50] Huld Thomas, Müller Richard, Gambardella Attilio. A new solar radiation database for estimating PV performance in Europe and Africa. Sol Energy 2012;86(6):1803–15.

[51] Holmgren Will, Calama-Consulting, Hansen Cliff, Anderson Kevin, Mikofski Mark, Lorenzo Antonio, et al. pvlib/pvlib-Python: v0.9.3. 2022, Zenodo.

[52] Holmgren William F, Hansen Clifford W, Mikofski Mark A. Pvlib Python: A Python package for modeling solar energy systems. J Open Source Softw 2018;3(29):884.

[53] Haas Sabine, Krien Uwe, Schachler Birgit, Bot Stickler, kyri-petrou, Zeli Velibor, et al. wind-python/windpowerlib: Silent improvements. 2021, Zenodo.

[54] Bhatt Arpit H, Tao Ling. Economic perspectives of biogas production via anaerobic digestion. Bioengineering 2020;7(3):74.

[55] Wiser Ryan, Rand Joseph, Seel Joachim, Beiter Philipp, Baker Erin, Lantz Eric, et al. Expert elicitation survey predicts 37% to 49% declines in wind energy costs by 2050. Nature Energy 2021;6(5):555–65.

[56] Christensen Adam. Assessment of hydrogen production costs from electrolysis: United States and Europe. In: International council on clean transportation. 2020, p. 1–73.

[57] Panos Evangelos, Kannan Ramachandran. The role of domestic biomass in electricity, heat and grid balancing markets in Switzerland. Energy 2016;112:1120–38.

[58] Petrović Stefan N, Karlsson Kenneth B. Residential heat pumps in the future Danish energy system. Energy 2016;114:787–97.

[59] Terlouw Tom, AlSkaif Tarek, Bauer Christian, van Sark Wilfried. Optimal energy management in all-electric residential energy systems with heat and electricity storage. Appl Energy 2019;254:113580.

[60] Zuberi MJS, Chambers J, Patel MK. Techno-economic comparison of technology options for deep decarbonization and electrification of residential heating. Energy Efficiency 2021;14:75.

[61] Fleiter Tobias, Steinbach Jan, Ragwitz Mario. Mapping and analyses of the current and future (2020 - 2030) heating/cooling fuel deployment (fossil/renewables) - Work package 1: Final energy consumption for the year 2012. Technical report, European commission under contract N° ENER/C2/2014-641, European Commission; 2016.
[62] IEA Paris. Global EV outlook 2022. Technical report, IEA, Paris; 2022.
[63] Sacchi R, Bauer C, Cox B, Mutel C. When, where and how can the electrification of passenger cars reduce greenhouse gas emissions? Renew Sustain Energy Rev 2022;162:112475.
[64] ecoinvent. Ecoinvent 3.9.1. 2022, [Accessed on Mo, 12 December 2022].
[65] Wernet Gregor, Bauer Christian, Steubing Bernhard, Reinhard Jürgen, Moreno-Ruiz Emilia, Weidema Bo. The ecoinvent database version 3 (Part I): Overview and methodology. Int J Life Cycle Assess 2016;21(9):1218–30.
[66] Mutel Chris. Brightway: An open source framework for life cycle assessment. J Open Sour Softw 2017;2(12):236.
[67] European Commission. Developer Environmental Footprint (EF). 2022.
[68] Madi H, Lytvynenko D, Jansohn P. Decarbonisation of geographical islands - The role of solar, wind and biomass. In: SyNERGY2022. 2022, [submitted conference paper].
[69] Madi Hossein. Investigations into the effects of biofuel contaminants on solid oxide fuel cells. Technical report, EPFL; 2016.
[70] Gurobi Optimization LLC. Gurobi optimizer reference manual. 2022.
[71] Mavromatidis Georgios, Orehounig Kristina, Bollinger L Andrew, Hohmann Marc, Marquant Julien F, Miglani Somil, et al. Ten questions concerning modeling of distributed multi-energy systems. Build Environ 2019;165:106372.
[72] Mancarella Pierluigi, Andersson Göran, Peças-Lopes JA, Bell Keith RW. Modelling of integrated multi-energy systems: Drivers, requirements, and opportunities. In: 2016 power systems computation conference. IEEE; 2016, p. 1–22.
[73] Victoria Marta, Zhu Kun, Brown Tom, Andresen Gorm B, Greiner Martin. The role of storage technologies throughout the decarbonisation of the sector-coupled European energy system. Energy Convers Manage 2019;201:111977.
[74] Halmschlager Daniel, Beck Anton, Knöttner Sophie, Koller Martin, Hofmann René. Combined optimization for retrofitting of heat recovery and thermal energy supply in industrial systems. Appl Energy 2022;305:117820.
[75] Sacchi R, Terlouw T, Siala K, Dirnaichner A, Bauer C, Cox B, et al. PRospective EnvironMental impact assement (premise): A streamlined approach to producing databases for prospective life cycle assessment using integrated assessment models. Renew Sustain Energy Rev 2022;160:112311.
[76] Gutierrez-Garcia Francisco, Arcos-Vargas Angel, Gomez-Exposito Antonio. Robustness of electricity systems with nearly 100% share of renewables: A worst-case study. Renew Sustain Energy Rev 2022;155:111932.
[77] Zheng Qipeng P, Wang Jianhui, Liu Andrew L. Stochastic optimization for unit commitment—A review. IEEE Trans Power Syst 2014;30(4):1913–24.
[78] Li Can, Grossmann Ignacio E. A review of stochastic programming methods for optimization of process systems under uncertainty. Front Chem Eng 2021;2:622241.
[79] Sen Souvik, Ganguly Sourav. Opportunities, barriers and issues with renewable energy development – A discussion. In: Renewable and sustainable energy reviews. 2017.
[80] Vasstrø m Mikaela, Lysgård Hans Kjetil. What shapes Norwegian wind power policy? Analysing the constructing forces of policymaking and emerging questions of energy justice. Energy Res Soc Sci 2021;102089.
[81] Yaqoot Mohammed, Diwan Parag, Kandpal Tara C. Review of barriers to the dissemination of decentralized renewable energy systems. Renew Sustain Energy Rev 2016;58:477–90.
[82] Juntunen Jouni K, Martiskainen Mari. Improving understanding of energy autonomy: A systematic review. Renew Sustain Energy Rev 2021;141:110797.
[83] McKenna Russell. The double-edged sword of decentralized energy autonomy. Energy Policy 2018;113:747–50.
[84] Weinand Jann Michael, Scheller Fabian, McKenna Russell. Reviewing energy system modelling of decentralized energy autonomy. Energy 2020;203:117817.